Engineering bone-like tissue *in vitro* using human bone marrow stem cells and silk scaffolds

Lorenz Meinel,[1,2,3] Vassilis Karageorgiou,[3] Sandra Hofmann,[3,4] Robert Fajardo,[5] Brian Snyder,[5] Chunmei Li,[3] Ludwig Zichner,[2] Robert Langer,[1] Gordana Vunjak-Novakovic,[1] David L. Kaplan[3]

[1]*Division of Health Sciences and Technology, Massachusetts Institute of Technology, E25-330, 45 Carleton Street, Cambridge, Massachusetts 02139*

[2]*University Hospital for Orthopaedic Surgery Friedrichsheim, Marienburgstrasse 2, 60528 Frankfurt, Germany*

[3]*Department of Biomedical Engineering, Tufts University, 4 Colby Street, Medford, Massachusetts 02155*

[4]*Department of Chemistry and Applied Biosciences, ETH Zurich, Winterthurerstrasse 190, 8057 Zurich, Switzerland*

[5]*Orthopaedic Biomechanics Laboratory, Beth Israel Deaconess Medical Center, Harvard University, Boston, Massachusetts 02215*

Received 24 February 2004; revised 21 May 2004; accepted 21 May 2004
Published online 12 August 2004 in Wiley InterScience (www.interscience.wiley.com). DOI: 10.1002/jbm.a.30117

Abstract: Porous biodegradable silk scaffolds and human bone marrow derived mesenchymal stem cells (hMSCs) were used to engineer bone-like tissue *in vitro*. Two different scaffolds with the same microstructure were studied: collagen (to assess the effects of fast degradation) and silk with covalently bound RGD sequences (to assess the effects of enhanced cell attachment and slow degradation). The hMSCs were isolated, expanded in culture, characterized with respect to the expression of surface markers and ability for chondrogenic and osteogenic differentiation, seeded on scaffolds, and cultured for up to 4 weeks. Histological analysis and microcomputer tomography showed the development of up to 1.2-mm-long interconnected and organized bonelike trabeculae with cuboid cells on the silk-RGD scaffolds, features still present but to a lesser extent on silk scaffolds and absent on the collagen scaffolds. The X-ray diffraction pattern of the deposited bone corresponded to hydroxyapatite present in the native bone. Biochemical analysis showed increased mineralization on silk-RGD scaffolds compared with either silk or collagen scaffolds after 4 weeks. Expression of bone sialoprotein, osteopontin, and bone morphogenetic protein 2 was significantly higher for hMSCs cultured in osteogenic than control medium both after 2 and 4 weeks in culture. The results suggest that RGD-silk scaffolds are particularly suitable for autologous bone tissue engineering, presumably because of their stable macroporous structure, tailorable mechanical properties matching those of native bone, and slow degradation. © 2004 Wiley Periodicals, Inc. J Biomed Mater Res 71A: 25–34, 2004

Key words: silk; stem cells; osteogenic; hydroxyapatite; tissue engineering

INTRODUCTION

In the United States, 2.5 million orthopedic and plastic reconstructions, including bone, cartilage, tendon, ligament, and breast, are performed annually.[1] Most bone repair procedures require a replacement structure to restore tissue function, including total substitutes (artificial joints), or tissue harvested from a second anatomic location of the same patient or from other patients and transplanted to the compromised area. Tissue engineering can provide an alternative to traditional treatment protocols by replacing living tissue with tissue grown *in vitro* that is designed and engineered to meet the needs of each individual patient and repair site.[2] In particular, tissue engineering of autologous bone using bone marrow derived human mesenchymal stem cells (hMSCs) can potentially avoid autologous grafting techniques. The hMSCs can proliferate in an undifferentiated state and with the appropriate extrinsic signals, differentiate into cells of various mesenchymal lineages, including cartilage and bone.[3–6]

To meet mechanical and functional requirements at the implant site, a mechanically stable slowly degrad-

Correspondence to: D. L. Kaplan; e-mail: david.Kaplan@tufts.edu

Contract grant sponsor: German Alexander Von Humboldt Foundation
Contract grant sponsor: National Institutes of Health; contract numbers: NIH R01DE13405-04, R01EB003210-01
Contract grant sponsor: National Science Foundation; contract grant number: NST DMR-0090384
Contract grant sponsor: NASA; contract grant number: NCC8-174

ing and biocompatible scaffold is required for bone engineering. Several studies have shown that hMSCs can differentiate along an osteogenic lineage and form three-dimensional (3D) bonelike tissue. However, these studies also highlight several important limitations. Some scaffolds (e.g., calcium phosphate) show limited ability to degrade,[7] whereas others degrade too fast.[8] Polymeric scaffolds used for bone tissue engineering, such as poly(lactic-*co*-glycolic acid) or poly-L-lactic acid can induce inflammation due to the acidity of their hydrolysis products.[9,10] Moreover, matching mechanical properties of native bone remains an issue with most polyesters.[11,12] Therefore, there is a need to identify alternate biomaterials to overcome these limitations and meet the challenging combination of biological, mechanical, and degradation features for bone tissue engineering.

To address the requirements of a mechanically robust and biocompatible material, 3D scaffolds were prepared from silk, a biomaterial known to have a wide range of native functions such as high strength netting to entrap insects and protective membranes to withstand environmental insults during development.[13] In addition, silk has a long history of use in medicine as sutures.[14,15] Recent studies with silk films and fiber matrices have shown a wide range of potential biomedical utility and the feasibility of hMSCs to attach to this biomaterial.[16–21] The goal of this study was to examine porous silk scaffolds for tissue-engineered human bone starting from hMSCs. The differentiation of hMSCs along osteogenic lineage and the formation of bonelike tissue were studied over 4 weeks *in vitro* on porous scaffolds made of silk (slow degrading), silk-RGD (slow degrading, enhanced cell attachment), and collagen (fast degrading) in control and osteogenic media.

MATERIALS AND METHODS

Materials

Bovine serum, RPMI 1640 medium, Dulbecco's modified eagle medium (DMEM), basic fibroblast growth factor (bFGF), transforming growth factor-β1 (TGF-β1) (R&D Systems, Minneapolis, MN), Pen-Strep, Fungizone, nonessential amino acids, and trypsin were from Gibco (Carlsbad, CA). Ascorbic acid phosphate, Histopaque-1077, insulin, dexamethasone, β-glycerolphosphate were from Sigma (St. Louis, MO). Collagen scaffolds (Ultrafoam) were from Davol (Cranston, RI). All other substances were of analytical or pharmaceutical grade and obtained from Sigma. Silkworm cocoons were kindly supplied by M. Tsukada (Institute of Sericulture, Tsukuba, Japan) and Marion Goldsmith (University of Rhode Island, Cranston, RI). BMP-2 was a gift from Wyeth Biopharmaceuticals, Andover, MA (Thomas Porter).

Scaffold preparation and decoration

Cocoons from *Bombyx mori* (Linne, 1758) were boiled for 1 h in an aqueous solution of 0.02 M Na_2CO_3 and rinsed with water to extract sericins. Purified silk was solubilized in 9 M LiBr solution and dialyzed (Pierce, Woburn, MA; MWCO 3500 g/mol) against water for 1 day and again against 0.1 M 2-[morpholino]ethanesulfonic acid (MES) (Pierce), 0.5 M NaCl, pH 6 buffer for another day. An aliquot of the silk solution was coupled with glycine-arginine-alanine-aspartate-serine (GRGDS) peptide to obtain RGD-silk. For coupling, COOH groups on the silk were activated by reaction with 1-ethyl-3-(dimethylaminopropyl)carbodiimide hydrochloride (EDC)/N-hydroxysuccinimide (NHS) solution for 15 min at room temperature.[13] To quench the EDC, 70 μL/mL β-mercaptoethanol was added. Then 0.5 g/L peptide was added and left for 2 h at room temperature. The reaction was stopped with 10 mM hydroxylamine. Silk solutions were dialyzed against water for 2 days. Silk and silk-RGD solutions were lyophilized and redissolved in hexafluoro-2-propanol (HFIP) to obtain a 17% (w/v) solution. Granular NaCl was weighed in a Teflon container and silk-HFIP solution was added at a ratio of 20:1 (NaCl:silk). HFIP was allowed to evaporate for 2 days, and NaCl-silk blocks were immersed in 90% (v/v) methanol for 30 min to induce a protein conformational transition to β-sheets.[22] Blocks were removed and dried, and NaCl was extracted out in water for 2 days, resulting in scaffolds with 98% porosity.[22] Disk-shaped scaffolds (5-mm diameter and 2-mm thick) were prepared by using a dermal punch (Miltey, Lake Success, NY) and autoclaved.

Iodination of GRYDS peptide

To assess the amount of bound RGD to the scaffolds, GRYDS peptide was iodinated with nonradioactive iodine to quantify the amount of bound peptide in the silk film surface by X-ray photoelectron spectrometer (XPS). The procedure involved first flushing of Sep-Pak C18 reverse phase cartridge (Waters) with 10 mL of an 80:20 mix of methanol: water and then flushing with 10 mL of 0.1 M PBS 0.5 M NaCl (pH = 6) buffer, as previously described.[13] Three IODOBEADS (Pierce) were rinsed once with 1 mL of PBS buffer. Eighty microliters of PBS and then 10 μL of 3.75 g/L NaI in PBS were added, and the activation was allowed for 5 min. Then, 1 mL of 0.1 g/L GRYDS peptide in PBS was added, and the reaction was allowed for 15 min. Beads were rinsed with PBS, and the peptide solution was injected into the C18 column followed by elution with 0, 20, 40, and 60% methanol in water solutions. Fractions were collected and analyzed at 280 nm. The iodination procedure was repeated with the same peptide through lyophilization of the desired fractions and resolubilizing in buffer to achieve the desired extent of iodination (1 atom of iodine per molecule of GRYDS). Iodinated peptide was coupled to silk matrices as described above for GRGDS.

Cell isolation, expansion, and characterization

The hMSCs were isolated by density gradient centrifugation from whole bone marrow (25 cm^3 harvests) obtained from Clonetics (Santa Rosa, CA). Briefly, samples of bone marrow were diluted in 100 mL of isolation medium (RPMI 1640 supplemented with 5% FBS). Bone marrow suspension (20-mL aliquots) was overlaid onto a polysucrose gradient (δ = 1,077 g/cm^3, Histopaque, Sigma, St. Louis, MO) and centrifuged at 800 g for 30 min at room temperature. The cell layer was carefully removed, washed in 10-mL isolation medium, pelleted, and the contaminating red blood cells were lysed in 5 mL of Pure-Gene Lysis solution. Cells were pelleted and suspended in expansion medium (DMEM, 10% FBS, 1 ng/mL bFGF) and seeded in 75-cm^2 flasks at a density of 5×10^4 cells/cm^2. The adherent cells were allowed to reach ~80% confluence (12–17 days for the first passage). Cells were trypsinized and replated every 6–8 days at ~80% confluence. The second passage (P2) cells were used if not otherwise stated.

The hMSCs were characterized with respect to 1) the expression of surface antigens and 2) the ability to selectively differentiate into chondrogenic or osteogenic lineages in response to environmental stimuli, as follows. The expression of the following six surface antigens: CD44 (hyaluronate receptor), CD14 (lipopolysaccharide receptor), CD31 (PECAM-1/endothelial cells), CD34 (sialomucin/hematopoietic progenitors), CD71 (transferring receptor/proliferating cells), and CD105 (endoglin) was characterized by fluorescence-activated cell sorting (FACS) analysis, as in our previous studies.[23,24] Cells were detached with 0.05% (w/v) trypsin, pelleted, and resuspended at a concentration of 1×10^7 cell/mL. Fifty-microliter aliquots of the cell suspension were incubated (30 min on ice) with 2 μL of each of the following antibodies: anti-CD44 and anti-CD14 conjugated with fluoresceine isothiocyanate (CD44-FITC, CD14-FITC), anti-CD31 conjugated with phycoerythrin (CD31-PE), anti-CD34 conjugated with allophycocyanine (CD34-APC), anti-CD71-APC, and anti-CD105 with a secondary rat-anti-mouse IgG-FITC antibody (all antibodies are from Neomarkers, Fremont, CA). Cells were washed, suspended in 100 μL of 2% formalin and subjected to FACS analysis.

To assess the potential of hMSC for osteogenic and chondrogenic differentiation, the cells were cultured in pellets in either control medium (DMEM supplemented with 10% FBS, Pen-Strep and Fungizone), chondrogenic medium (control medium supplemented with 0.1 mM nonessential amino acids, 50 μg/mL ascorbic acid-2-phosphate, 10 nm dexamethasone, 5 μg/mL insulin, 5 ng/mL TGF β1), or osteogenic medium (control medium supplemented with 50 μg/mL ascorbic acid-2-phosphate, 10 nm dexamethasone, 7 mM β-glycerolphosphate, and 1 μg/mL BMP-2). Cells were isolated from monolayers by trypsin and washed in PBS. Aliquots containing 2×10^5 cells were centrifuged at 300 g in 2-mL conical tubes and allowed to form compact cell pellets over 24 h in an incubator (5% CO_2, 37°C). Medium was changed every 2–3 days. After 4 weeks of culture, pellets were washed twice in PBS, fixed in 10% neutral buffered formalin (24 h at 4°C), embedded in paraffin, and sectioned (5-μm thick). Sections were stained for general evaluation [hematoxilin and eosin (H&E)], the presence of glycosaminoglycan (GAG) (safranin O/fast green), and mineralized tissue (according to von Kossa in 5% $AgNO_3$ for 1 h, exposed to a 60 W bulb, and counterstained with fast red). In addition, the amounts of GAG and calcium were measured as described below by using n = five or six pellets per sample.

Pellet culture

For pellet culture, 2×10^5 cells were centrifuged at 300 g for 10 min at 4°C. The medium was aspirated and replaced with osteogenic, chondrogenic, or control medium. Control medium was DMEM supplemented with 10% FBS, Pen-Strep, and Fungizone. Chondrogenic medium was control medium further supplemented with 0.1 mM nonessential amino acids, 50 μg/mL ascorbic acid-2-phosphate, 10 nm dexamethasone, 5 μg/mL insulin, and 5 ng/mL TGF β1. Osteogenic medium was control medium further supplemented with 50 μg/mL ascorbic acid-2-phosphate, 10 nm dexamethasone, 7 mM β-glycerolphosphate, and 1 μg/mL BMP-2.

Tissue culture

For cultivation on scaffolds, P2 hMSCs were suspended in liquid Matrigel (7×10^5 cells per scaffold in 10 μL Matrigel) while working on ice to prevent gelation, and the suspension was seeded onto prewetted scaffolds (overnight incubation in DMEM). Seeded constructs (in culture dishes, without added medium) were placed in an incubator at 37°C for 15 min to allow gel hardening, and 5 mL osteogenic or control medium was subsequently added. Half of the medium was replaced every 2–3 days.

Biochemical analysis

Constructs were harvested after 2 and 4 weeks of cultivation and processed for biochemical analyses and histology. For DNA analysis, $N = 3$ or 4 scaffolds per group and time point were disintegrated by using steel balls and a Minibead-beater (Biospec, Bartlesville, OK). DNA content was measured by using the PicoGreen assay (Molecular Probes, Eugene, OR), according to the protocol of the manufacturer. Samples were measured fluorometrically at an excitation wavelength of 480 nm and an emission wavelength of 528 nm. Sulfated GAG content of cell pellets (n = 5), was assessed as previously described.[25] Briefly, pellets were frozen, lyophilized for 3 days, weighed, and digested for 16 h at 60°C with 1 mg/cm^3 papain solution in buffer (50 mM TRIS, 1 mM ethylenediamine tetraacetic acid, EDTA, 1 mM iodoacetamide, 10 $\mu g/cm^3$ pepstatin-A) using 1 cm^3 enzyme solution per 4- to 10-mg dry weight (mg dw) of the sample.[26] GAG content was determined spectrophotometrically (Perkin Elmer, Oak Bridge, IL) at 525 nm after binding to the dimethylmethylene blue dye.[27] To measure the amount of calcium, samples (n = 4 or 5) were extracted

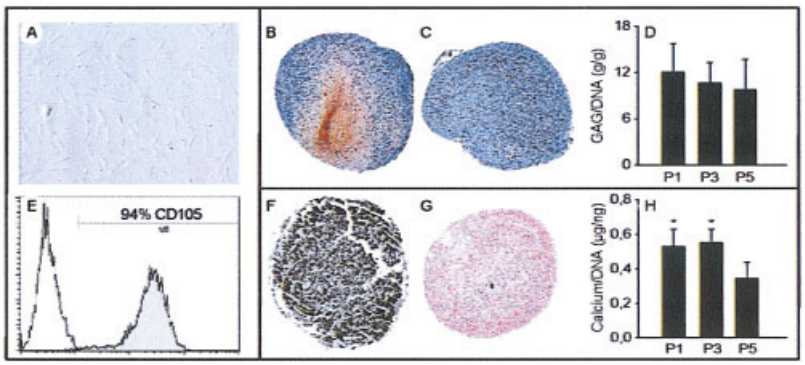

Figure 1. Characterization as hMSCs. (A) Phase-contrast photomicrographs of passage 2 hMSCs at an original magnification of ×20. (B–D) Characterization of chondrogenic differentiation in pellet culture. Pellets were either cultured in chondrogenic medium (B) or control medium (C). Pellet diameter is ~2 mm, and pellets were stained with safranin O/Fast Red. (D) Sulfated GAG/DNA (μg/μg) deposition of passages 1, 3, and 5 hMSCs after 4 weeks. Data represent the average ± SD of five pellets. (B) Endoglin expression (CD105) of passage 2 hMSCs. (F–H) Characterization of osteoblastic differentiation in pellet culture either treated in osteogenic (F) or in control medium (G) and stained according to von Kossa. Pellet diameter is ~2 mm. (H) Calcium deposition/DNA (μg/ng) of passages 1, 3, and 5 hMSCs pellet culture. Passage 1 and 3 cells deposited significantly more calcium/DNA than passage 5 cells ($p < 0.05$), and data represent the average ± SD of five pellets.

twice with 0.5 mL 5% trichloroacetic acid. Calcium content was measured spectrophotometrically at 575 nm after the reaction with o-cresolphthalein complexone according to the manufacturer's protocol (Sigma). Alkaline phosphatase activity was measured by using a biochemical assay from Sigma based on conversion of p-nitrophenyl phosphate to p-nitrophenol, which was measured spectrophotometrically at 410 nm.

RNA isolation, real-time reverse transcription polymerase chain reaction (real-time RT-PCR)

Fresh constructs (n = 3 or 4 per group and time point) were transferred into 2-mL plastic tubes, and 1.5 mL Trizol was added. Constructs were disintegrated by using steel balls and a Minibead beater. Tubes were centrifuged at 12,000 g for 10 min, and the supernatant was transferred to a new tube. Chloroform (190 μL) was added to the solution and incubated for 5 min at room temperature. Tubes were again centrifuged at 12,000 g for 15 min, and the upper aqueous phase was transferred to a new tube. One volume of 70% ethanol (v/v) was added and applied to an RNeasy mini spin column (Qiagen, Hilden, Germany). The RNA was washed and eluted according to the manufacturer's protocol.

The RNA samples were reverse transcribed in cDNA using oligo (dT)-selection according to the manufacturer's protocol (Superscript Preamplification System, Life Technologies, Gaithersburg, MD). Collagen type II gene expression was quantified by using the ABI Prism 7000 Real Time PCR system (Applied Biosystems, Foster City, CA). PCR reaction conditions were 2 min at 50°C, 10 min at 95°C, 50 cycles at 95°C for 15 s, and 1 min at 60°C. The expression data were normalized to the expression of the housekeeping gene, glyceraldehyde-3-phosphate-dehydrogenase (GAPDH). Probes were labeled at the 5′ end with fluorescent dye FAM (VIC for GAPDH) and with the quencher dye TAMRA at the 3′ end. Primer sequences for the human GAPDH gene were: forward primer 5′-ATG GGG AAG GTG AAG GTC G-3′, reverse primer 5′-TAA AAG CCC TGG TGA CC-3′, probe 5′-CGC CCA ATA CGA CCA AAT CCG TTG AC-3′. Primers and probes for osteopontin, bone sialoprotein (BSP), and bone morphogenic protein 2 (BMP-2) were purchased from Applied Biosciences (Assay on Demand #Hs00167093 mL (osteopontin), Hs 00173720 mL (BSP), and Hs 00214079 mL (BMP-2)).

Histology

For histology, constructs were fixed in neutral-buffered formalin (24 h at 4°C), dehydrated in graded ethanol solutions, embedded in paraffin, bisected through the center, and cut into 5-μm-thick sections. To stain for cartilage differentiation in the pellet culture (Fig. 1), sections were treated with eosin for 1 min, fast green for 5 min, and 0.2% aqueous safranin O solution for 5 min, rinsed with distilled water, dehydrated through xylene, mounted, and placed under a coverslip.[28] Staining for bone differentiation was according to von Kossa.[29]

Microcomputerized tomography (micro-CT)

For the visualization of bone distribution, constructs were analyzed by using a micro-CT20 imaging system (Scanco Medical, Bassersdorf, Switzerland) providing a resolution of 34 μm in the face and 250 μm in the cross direction of the scaffold. A constrained Gaussian filter was used to suppress noise. Mineralized tissue was segmented from nonmineralized tissue using a global thresholding procedure. All samples were analyzed by using the same filter width (0.7), filter support (1), and threshold protocol as previously described.[23,30]

X-ray diffraction (XRD)

XRD patterns of scaffolds before and after bone formation were obtained by means of Bruker D8 Discover X-ray diffractometer with GADDS multiwire area detector. Wide angle X-ray diffraction (WAXD) experiments were performed by using CuKa radiation (40 kV and 20 mA) and 0.5-mm collimator. The distance between the detector and the sample was 47 mm.

Statistical analysis

Statistical analysis of data was performed by one-way analysis of variance (ANOVA) and Tukey-Kramer procedure for post hoc comparison using SigmaStat 3.0 for Windows. $p < 0.05$ was considered statistically significant.

RESULTS

Characterization of hMSC

The hMSCs exhibited a spindle-shaped and fibroblast-like morphology [Fig. 1(A)]. FACS analysis showed that >90% of the cells were positive for CD105, a putative marker for mesenchymal stem cells [Fig. 1(E)]. The chondrogenic potential of second passage (P2) cells was evidenced by evenly red stained areas indicating GAG deposition in the center of the pellets [Fig. 1(B)]; pellets incubated with either control or osteogenic medium showed no red staining [Fig 1(C)]. These findings were corroborated by the analysis of sulphated GAG content per unit DNA for chondrogenic differentiation of P1, P3, and P5 cells, with no significant differences between the passaages [Fig. 1(D)]. Osteogenic potential of the cells was shown by the spatially uniform deposition of calcified matrix [Fig. 1(F)]; pellets incubated in control medium or chondrogenic medium did not show any black or dark brown staining, thus indicating the absence of mineralization [Fig. 1(G)]. Calcium content per unit DNA was analyzed to quantify the histological observations for osteogenic differentiation for P1, P3, and P5 cells [Fig. 1(H)]. P1 and P3 cells deposited significantly more calcium per DNA than P5 cells ($p < 0.05$). It is important to note that hMSCs underwent chondrogenic differentiation only when cultured in chondrogenic medium and osteogenic differentiation only when cultured in osteogenic medium.

Effect of scaffold material on osteogenic differentiation of hMSCs

Calcium content increased on silk and RGD-silk scaffolds but not on collagen [Fig. 2(A)], a pattern

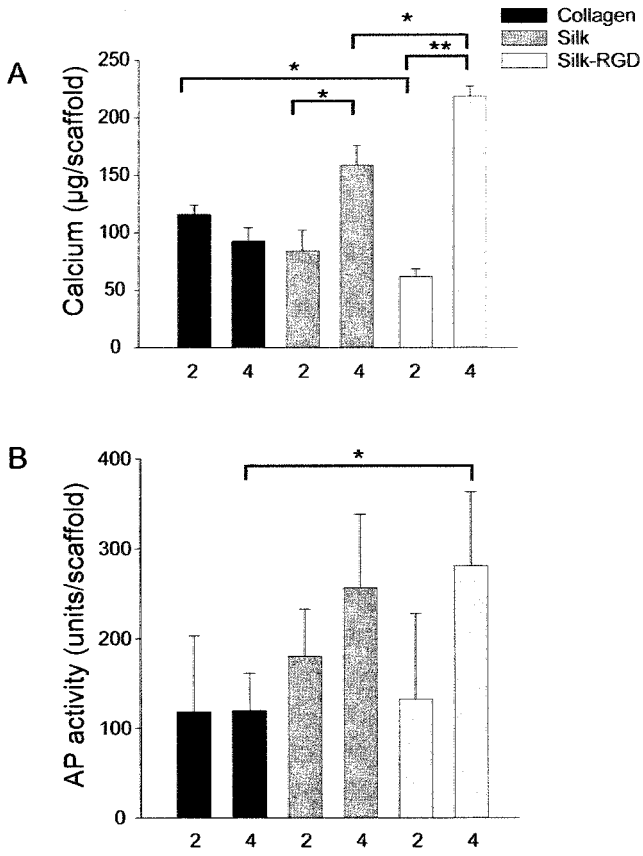

Figure 2. Biochemical characterization of hMSC differentiation on collagen, silk, and silk-RGD scaffolds after 2 and 4 weeks in osteogenic culture medium. (A) Calcium deposition per scaffold and (B) alkaline phosphatase (AP) activity per scaffold. Data are represented as the average ± SD of three or four constructs, and asterisks indicate statistically significant differences (*$p < 0.05$; **$p < 0.01$).

consistent with the respective differences in degradation rates of the three scaffolds. In particular, advanced biodegradation of collagen resulted in a wet weight of ~17% of the initial weight after 4 weeks of culture.[23] After 2 weeks of culture, the amounts of calcium were comparable for all three groups. After 4 weeks of culture, the amounts of calcium on silk and RGD-silk scaffolds were markedly and significantly larger compared with collagen scaffolds ($p < 0.05$ and $p < 0.02$, respectively [Fig. 2(A)]. In contrast to collagen scaffolds, which tended to lose calcium with time in culture, significantly more calcium was deposited on silk and RGD-silk scaffolds after 4 weeks of culture compared with 2 weeks of culture [$p < 0.05$; Fig. 2(A)]. In addition, the amount of calcium on RGD-silk scaffolds was significantly higher than that on silk scaffolds [$p < 0.05$ Fig. 2(A)]. Essentially the same pattern was observed for the alkaline phosphatase (AP) activity of hMSCs in tissue constructs based on collagen, silk, and RGD-silk scaffolds [Fig. 2(B)].

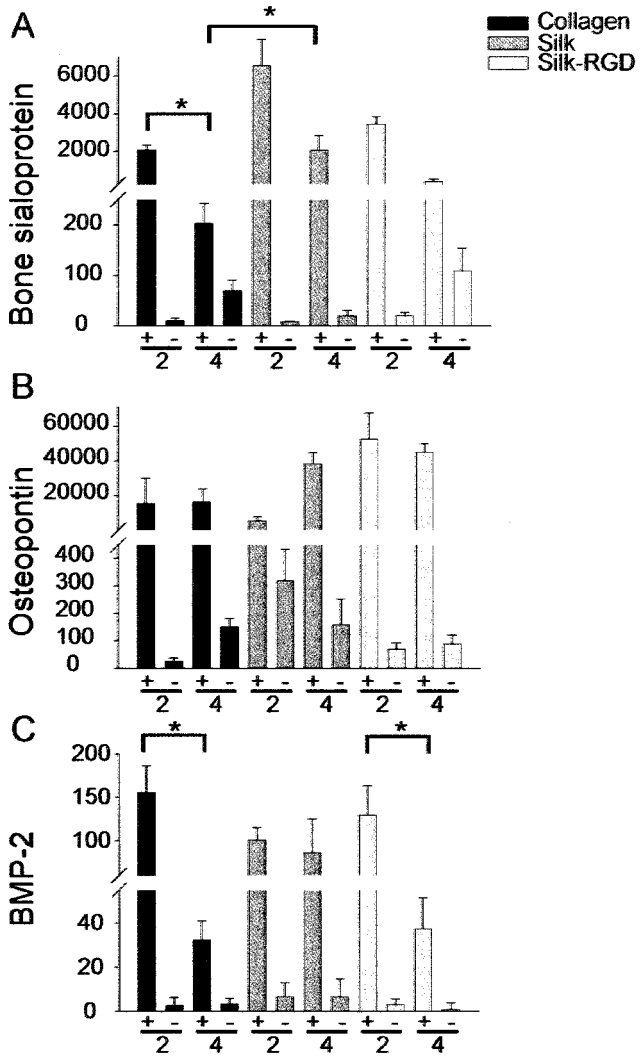

Figure 3. Transcript levels from cells cultured on collagen, silk, and silk-RGD matrices in osteogenic medium (+) and control medium (−) after 2 and 4 weeks in culture. (A) Expression of bone sialoprotein, (B) osteopontin, and (C) BMP-2. Data are shown relative to the expression of the respective gene in hMSCs before seeding and is the average ± SD of three or four constructs.

Gene expression of bone sialoprotein, osteopontin and BMP-2 mRNA

Strong transcript levels of all three bone markers studied [bone sialoprotein (BSP), osteopontin and BMP-2] were observed only for hMSCs cultured in osteogenic medium (Fig. 3). For all three scaffolds, a significant decline in BSP transcript levels was observed between 2 and 4 weeks of cultivation ($p < 0.05$) [Fig. 3(A)]. At both time points, BSP expression was higher on silk and RGD-silk than on collagen scaffolds [Fig. 3(A)] ($p < 0.05$) after 4 weeks ($p < 0.05$).

Osteopontin expression in hMSCs cultured in osteogenic medium was comparable for all three scaffolds at both time points [Fig. 3(B)], and the measured transcript levels were statistically indistinguishable from those measured in freshly isolated hMSCs (represented by the baseline).

Bone morphogenetic protein 2 (BMP-2) expression was up-regulated 100–150-fold after 2 weeks on all scaffolds cultured in osteogenic medium compared with the hMSCs before seeding [Fig. 3(C)]. Fewer transcripts were found after 4 weeks on collagen and silk-RGD scaffolds ($p < 0.05$), whereas silk scaffolds maintained their expression levels [Fig. 3(C)]. After 4 weeks of culture, the transcript levels of BMP-2 were comparable for the three scaffolds.

Histogenesis of bone-like tissue

Collagen-based constructs contained mineralized spots after 2 weeks of cultivation [Fig. 4(A)]. Open areas of the lattice were filled with randomly oriented fibroblasts embedded in a fibrous matrix as seen in H&E staining [Fig. 4(B)]. Enlarged cuboidal cells with an osteoblast-like morphology were also observed at random locations [Fig. 4(B)]. After 4 weeks, calcification occurred in locations that coalesced and formed clusters of mineralized matrix [Fig. 4(C)]. Fewer cells were present after 4 weeks than after 2 weeks, and a

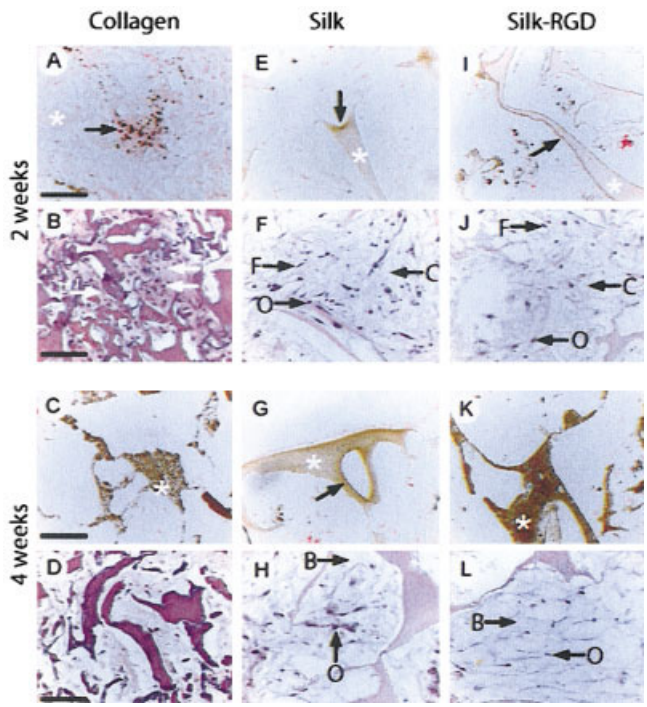

Figure 4. Histological sections taken from collagen (A–D), silk (E–H), and silk-RGD (I–L) scaffolds cultured for 2 weeks (upper panel) or 4 weeks (lower panel) in osteogenic medium. Von Kossa staining (A, C, E, G, I, K) and H&E staining (B, D, F, H, J, L); bar length = 70 μm. Arrows indicate calcification; asterisks indicate polymer. O = osteoblast-like cell; F = fibroblast-like cell; B = collagen-like bundles.

mixture of osteoblast-like and fibroblast-like cells was observed [Fig. 4(D)].

Silk-based constructs had mineralization foci that were appositional to the scaffold lattice and occurred in distinct spots [Fig. 4(E)]. The void areas of the matrix were filled with randomly oriented collagen-like fibers, and some fibroblasts and osteoblast-like cells were also found, predominantly adjacent to the silk [Fig. 4(F)]. After 4 weeks, mineral deposition was advanced, especially in the peripheral region [Fig. 4(G)]. Changes in the extracellular matrix were confined to restricted areas ($\sim 50 \times 50$ μm) with parallel oriented collagen bundles surrounded by areas with randomly oriented collagen bundles. Increased numbers of osteoblast-like cells with a cuboidal or columnar morphology were observed, and some of the cells were in contact via short processes [Fig. 4(H)].

In silk-RGD-based constructs, mineralization occurred in a mode similar to the silk-based constructs, appositional to the scaffold lattice [Fig. 4(I)]. After 2 weeks of culture in osteogenic medium, the scaffold was filled with connective tissue comprised of randomly oriented collagen-like fibers, fibroblasts, and cuboidal osteoblast-like cells connected via cellular processes [Fig. 4(J). After 4 weeks of culture, mineralization on the silk-RGD scaffolds was more extensive than on either silk or collagen scaffolds [Fig. 4(K)]. The void area between the lattices was completely filled with extracellular matrix, consisting of parallel oriented collagen bundles, osteoblast-like cells, and few cells with fibroblast-like morphology. The cells seemed to be interconnected via long processes [Fig. 4(L)].

Microstructure of engineered bone

Bone deposition was imaged after 4 weeks of culture in osteogenic medium with microcomputerized tomography (micro-CT) (Fig. 5). In collagen-based constructs, mineralized clusters were small, discrete, and present mainly at the outer rim of the constructs [Fig. 5 (A,B)]. Biodegradation resulted in a concave shape of the scaffold and a decrease in diameter and thickness by ~30% from the original. The silk-RGD scaffold showed advanced mineralization, with newly formed bone at the top and bottom but not in the center of the construct [Fig. 5(C,D)]. The scaffold size remained unchanged during the experiment, indicating no substrate degradation during the time frame of the experiment [Fig. 5(C)]. The calcified rods formed interconnected lattices that were up 1.2 mm long. These interconnected lattices formed trabecular-like geometries, encircling hexagonal voids [Fig. 5(D) and insert 5(C)].

To verify the bonelike nature of the deposited tissue, we compared XRD patterns of engineered and native bone, to visualize poorly crystalline hydroxyapatite (p.c. HA) as predominantly present in bone.[31] XRD analysis from the tissue-engineered bonelike tissue on silk, collagen, and silk-RGD (Fig. 6) revealed the same structure of p.c. HA.

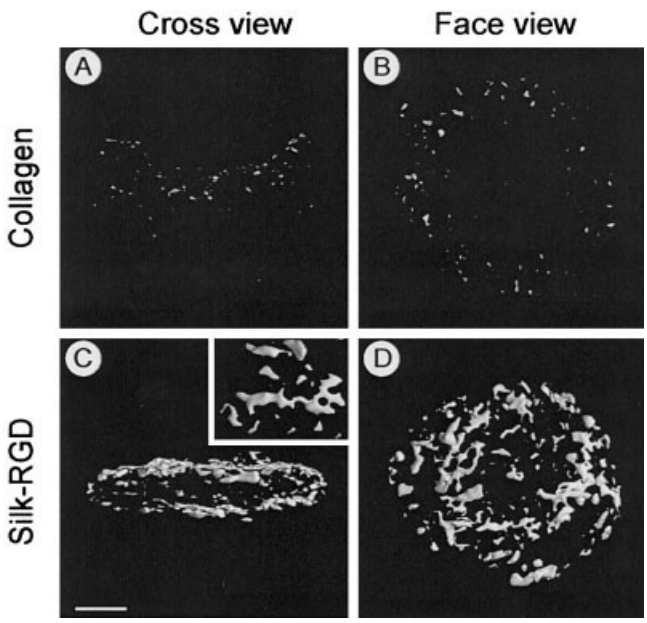

Figure 5. Micro-CT images taken from collagen (A, B), and silk-RGD scaffolds (C, D). Insert in C is a magnification from D. Bar length = 1.1 mm.

DISCUSSION

We report tissue engineering of bone-like structures based on hMSCs (isolated from bone marrow, expanded in culture and characterized) and porous silk scaffolds (made from biodegradable silk and in some cases modified by RGD sequences). When cultured on silk scaffolds in osteogenic medium (but not in control medium), hMSCs expressed bone markers (bone sialoprotein, osteopontin, and BMP-2) and accumulated bone-like matrix that contained alkaline phosphatase and mineral and consisted of bone trabeculae. The progression and extent of osteogenesis were markedly and significantly higher, according to all measured parameters, for silk and RGD-silk scaffolds compared with collagen scaffolds. These differences could be attributed, at least in part, to the porous and stable structure, mechanical properties, and slow degradation of silk scaffolds. Taken together, these data suggest that hMSCs cultured on appropriate scaffolds can form the basis for tissue engineering of autologous human bone grafts for scientific studies and eventual clinical applications.

The hMSCs are an obvious source of cells for autol-

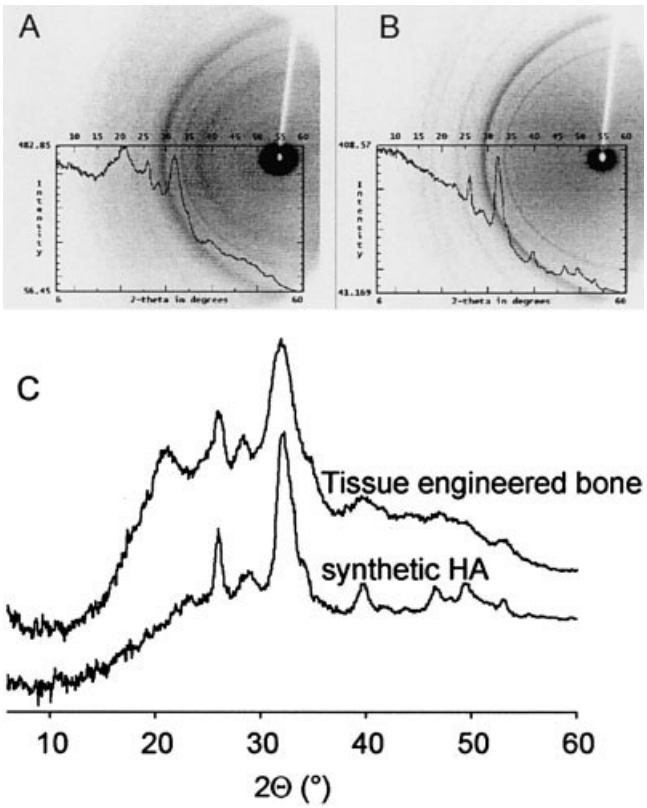

Figure 6. XRD patterns generated by (A) tissue engineered bone on silk-RGD, (B) poorly crystalline hydroxyapatite (p.c. HA), and (C) the overlay of the XRD patterns of tissue engineered bone and p.c. HA minus the XRD pattern of air, respectively.

ogous bone tissue engineering. They proliferate and differentiate *in vitro,* can be easily isolated from bone marrow aspirates, and have a documented potential for osteogenic and chondrogenic differentiation.[3–5,32] The osteogenic pathway has been proposed to be the default lineage of this population of cells.[33] The isolated and expanded hMSCs were positive for the putative stem cell marker CD105/endoglin[34] and had a capacity for selective differentiation into either cartilage- or bone-forming cells [Fig. 1(E)]. The expanded cells could be induced to undergo either chondrogenic or osteogenic differentiation via medium supplementation with chondrogenic or osteogenic factors, respectively [Fig. 1(B,C) and Fig. 1(F,G), respectively]. No notable difference in cell differentiation capacity over three passages in culture was observed; however, calcium deposition of P5 cells was significantly reduced compared with P1 and P3 cells [Fig. 1(D,H)]. Therefore, P2 hMSCs used in this study retained osteogenic and chondrogenic differentiation potential, which made them a suitable cell source for bone tissue engineering.

Scaffold chemistry and surface modification had a significant impact on mineralization of the matrices. Calcium deposition on collagen scaffolds declined after 4 weeks, an effect correlated with the biodegradation of the collagen scaffold.[23] Ideally, a scaffold provides a suitable mechanical match until gradually replaced by the newly deposited bone. Although some bone deposition was already present after 2 weeks in culture [Fig. 2(A)], the biodegradation of collagen was too rapid to allow isomorphous replacement with newly formed bone. Histological evaluation showed a progression in bone deposition on collagen scaffolds between week 2 and 4, although total calcium per scaffold decreased because of biodegradation.

Unmodified collagen did not retain its structure leading to collapsed fragments intermingled with the connective tissue [Fig. 4(D,J)]. Presumably, the eroding frame did not allow the bone clusters to connect; therefore, randomly distributed mineralized clusters were scattered mainly at the rim of the scaffold, also leading to transport limitations in the center of the collapsed structure (Fig. 5). In one of our previous studies, collagen scaffolds were crosslinked (CL-collagen) to reduce the rate of biodegradation to understand the significance of biodegradation on the decline in calcium content.[23] The CL-collagen did not show substantial degradation, whereas the natural polymer degraded and wet weight after 4 weeks in culture was about 5 times less as the initial weight. Similarly, calcium content on the CL-collagen was 6 times higher than the untreated and natural polymer. These previously related data suggest that the observed loss in calcium content on the natural collagen was mainly due to rapid degradation of the scaffold. However, chemical crosslinking may cause cytotoxic effects and have reduced biocompatibility compared with native materials.[35] Furthermore, silk-based materials can provide a broader range of mechanical properties than collagen-based materials, which may be a substantial advantage to meet physiological needs at the implantation site.[17] Because of these constraints and the focus of this study to compare natural polymers, crosslinked collagen was not included in the present study.

The introduction of RGD moieties by covalent binding to silk surfaces resulted in significantly increased calcium deposition than either nondecorated silk or collagen [Fig. 2(A)]. This result is consistent with our previous studies of silk films decorated with RGD.[13] It is interesting that bone formation on silk-RGD scaffolds resulted in interconnected trabeculae of bonelike tissue (Fig. 5). The trabeculae encircle hexagonal void areas, which were in the range of the pore sizes of the silk scaffolds. Histological evaluation corroborated this evidence, documenting that new bonelike tissue was deposited appositionally to the silk scaffold lattice [Fig. 4(G,K)]. These data suggest that the silk scaffold geometry may predetermine the geometry of the engineered bone.

Calcium deposition was mainly on the top and bottom of the scaffold (Fig. 5). Similar to most previous

studies, it is likely that diffusional limitations associated with mass transport have limited successful efforts to engineer compact and continuous bone structures.[36,37] Bioreactors can help overcome these limitations, by enhanced supply of oxygen, nutrients, metabolites, and regulatory molecules to the center of the scaffolds.[38] Because silk biodegradation is slow, the scaffolds provide a robust network likely to withstand medium flow used in most bioreactors without the loss of mechanical integrity.

The similarity in XRD patterns between p.c. HA and the engineered tissue suggested the bonelike nature of the deposited interconnected trabeculae (Fig. 6). From early diffraction measurements, it was concluded that bone mineral is a two-phase system, one of which was p.c. HA and the other an amorphous calcium phosphate, which makes up <10% of the mineralized bone.[39] However, more recent studies could not detect amorphous calcium phosphate even in embryonic bone.[40,41] Substantial differences in the organization of the extracellular matrix were observed on the silks after 2 and 4 weeks of culture in osteogenic medium. After 4 weeks, dense connective tissue filled the voids of the silk and silk-RGD lattice in which cuboidal osteoblast-like cells were in contact with one another via long tapering processes. The intercellular space was occupied with organized bundles of collagens [Fig. 4(K,L)]. This was accompanied by strong induction of gene expression for bone sialoprotein (BSP) (Fig. 3). BSP constitutes about 15% of the noncollagenous proteins found in the mineralized compartment of young bone and supports cell attachment through both RGD-dependent and RGD-independent mechanisms, with a high affinity for hydroxyapatite.[42] The strong up-regulation of both genes in response to BMP-2 has been reported in previous studies.[43,44] The up-regulated expression of BSP reflects the strong induction of extracellular matrix protein production, which is seen in the histological sections (Fig. 4). Osteopontin expression was similarly increased after 2 and 4 weeks on all scaffolds. Osteopontin regulates cell adhesion, migration, survival, and calcium crystal formation, playing a role in biomineralization and early osteogenesis.[45] Therefore, the increased expression of osteopontin corroborates the advanced mineralization progress evident after 2 weeks in culture.

In summary, tissue-engineered trabecular bone-like morphologies were created *in vitro* by culturing hMSCs cultured in osteogenic medium on porous silk scaffolds. This was accompanied by the production of an organized extracellular matrix. The decoration of silk scaffolds with RGD sequences resulted in increased calcification and a more structured extracellular matrix. Collagen scaffolds could not generate similar outcomes because of the rapid rate of degradation. An envisioned scenario to obtain large tissue-engineered bone with an organized geometry on natural noncrosslinked polymers would involve the cultivation of hMSCs seeded on silk-RGD scaffolds in conjunction with bioreactors.

This work was supported by the German Alexander Von Humboldt Foundation (Feodor-Lynen Fellowship to LM), the National Institutes of Health (to DLK), the National Science Foundation (to DLK) and NASA (to GV-N). We thank Annette Shepard-Barry, Division of Pathology, New England Medical Center, Tufts University, for her help with the immunohistochemistry.

References

1. Lysaght MJ, Nguy NA, Sullivan K. An economic survey of the emerging tissue engineering industry. Tissue Eng 1998;4:231–238.
2. Vacanti JP, Langer R. Tissue engineering: the design and fabrication of living replacement devices for surgical reconstruction and transplantation. Lancet 1999;354 (Suppl 1):S132–S134.
3. Friedenstein AJ. Precursor cells of mechanocytes. Int Rev Cytol 1976;47:327–359.
4. Friedenstein AJ, Chailakhyan RK, Gerasimov UV. Bone marrow osteogenic stem cells: in vitro cultivation and transplantation in diffusion chambers. Cell Tissue Kinet 1987;20:263–272.
5. Caplan AI. The mesengenic process. Clin Plast Surg 1994;21: 429–435.
6. Mackay AM, Beck SC, Murphy JM, Barry FP, Chichester CO, Pittenger MF. Chondrogenic differentiation of cultured human mesenchymal stem cells from marrow. Tissue Eng 1998;4:415–428.
7. Ohgushi H, Okumura M, Masuhara K, Goldberg VM, Davy DT, Caplan AI. Calcium phosphate block ceramic with bone marrow cells in a rat long bone defect. In: Yamamuro T, Hench LL, Wilson J, editors. CRC handbook of bioactive ceramics. Vol. 2. Boca Raton, FL: CRC Press; 1992. pp 235–238.
8. Petite H, Viateau V, Bensaid W, Meunier A, de Pollak C, Bourguignon M, Oudina K, Sedel L, Guillemin G. Tissue-engineered bone regeneration. Nat Biotechnol 2000;18:959–963.
9. Athanasiou KA, Niederauer GG, Agrawal CM. Sterilization, toxicity, biocompatibility and clinical applications of polylactic acid/polyglycolic acid copolymers. Biomaterials 1996;17:93–102.
10. Hollinger JO, Brekke J, Gruskin E, Lee D. Role of bone substitutes. Clin Orthop 1996;324:55–65.
11. Harris LD, Kim BS, Mooney DJ. Open pore biodegradable matrices formed with gas foaming. J Biomed Mater Res 1998; 42:396–402.
12. Suh H. Recent advances in biomaterials. Yonsei Med J 1998;39: 87–96.
13. Sofia S, McCarthy MB, Gronowicz G, Kaplan DL. Functionalized silk-based biomaterials for bone formation. J Biomed Mater Res 2001;54:139–148.
14. Lange F. Über die Sehenplastik. Verh Dtsch Orthop Ges 1903; 2:10–12.
15. Lange F. Künstliche Bänder aus Seide. Münch Med Wochenschr 1907;17:834–836.
16. Perez-Rigueiro J, Viney C, Llorca J, Elices M. Silkworm silk as an engineering material. J Appl Poly Sci 1998;70:2439–2447.
17. Altman GH, Diaz F, Jakuba C, Calabro T, Horan RL, Chen J, Lu H, Richmond J, Kaplan DL. Silk-based biomaterials. Biomaterials 2003;24:401–416.

18. Altman GH, Horan RL, Lu HH, Moreau J, Martin I, Richmond JC, Kaplan DL. Silk matrix for tissue engineered anterior cruciate ligaments. Biomaterials 2002;23:4131–4141.
19. Kaplan DL. Spiderless spider webs. Nat Biotechnol 2002;20: 239–240.
20. Chen J, Altman GH, Karageorgiou V, Horan RL, Collette A, Volloch V, Colabro T, Kaplan DL. Human bone marrow stromal cells and ligament fibroblasts responses on RGD-modified silk fibres. J Biomed Mater Res 2003;67A:559–570.
21. Minoura N, Aiba S, Gotoh Y, Tsukada M, Imai Y. Attachment and growth of cultured fibroblast cells on silk protein matrices. J Biomed Mater Res 1995;29:1215–1221.
22. Nazarov C, Jin HJ, Kaplan DL. Porous 3-d scaffolds from regenerated silk fibroin. Biomacromolecules 2004;5:718–726.
23. Meinel L, Kareourgiou V, Fajardo R, Snyder B, Shinde-Patil V, Zichner L, Kaplan D, Langer R, Vunjak-Novakovic G. Bone tissue engineering using human mesenchymal stem cells: effects of scaffold material and medium flow. Ann Biomed Eng 2003;32:112–122.
24. Meinel L, Hofmann S, Karageorgiou V, Kirker-Head C, Zichner L, Langer R, Vunjak-Novakovic G, Kaplan D. Inflammatory responses in vivo and in vitro to silk and collagen films. Biomaterials 2003. Forthcoming.
25. Martin I, Obradovic B, Freed LE, Vunjak-Novakovic G. Method for quantitative analysis of glycosaminoglycan distribution in cultured natural and engineered cartilage. Ann Biomed Eng 1999;27:656–662.
26. Freed LE, Marquis JC, Nohria A, Emmanual J, Mikos AG, Langer R. Neocartilage formation in vitro and in vivo using cells cultured on synthetic biodegradable polymers. J Biomed Mater Res 1993;27:11–23.
27. Farndale RW, Buttle DJ, Barrett AJ. Improved quantitation and discrimination of sulphated glycosaminoglycans by use of dimethylmethylene blue. Biochim Biophys Acta 1986;883:173–177.
28. Rosenberg L. Chemical basis for the histological use of safranin O in the study of articular cartilage. J Bone Joint Surg Am 1971;53:69–82.
29. Sheehan DC, Hrapchak BB. Theory and practice of histotechnology. St. Louis, MO: C. V. Mosby Co.; 1973. pp xi, 218.
30. Muller R, Hildebrand T, Ruegsegger P. Non-invasive bone biopsy: a new method to analyse and display the three-dimensional structure of trabecular bone. Phys Med Biol 1994;39:145–164.
31. Harper RA, Posner AS. Measurement of non-crystalline calcium phosphate in bone mineral. Proc Soc Exp Biol Med 1966; 122:137–142.
32. Pittenger MF, Mackay AM, Beck SC, Jaiswal RK, Douglas R, Mosca JD, Moorman MA, Simonetti DW, Craig S, Marshak DR. Multilineage potential of adult human mesenchymal stem cells. Science 1999;284:143–147.
33. Banfi A, Bianchi G, Notaro R, Luzzatto L, Cancedda R, Quarto R. Replicative aging and gene ;Expression in long-term cultures of human bone marrow stromal cells. Tissue Eng 2002;8: 901–910.
34. Barry FP, Boynton RE, Haynesworth S, Murphy JM, Zaia J. The monoclonal antibody SH-2, raised against human mesenchymal stem cells, recognizes an epitope on endoglin (CD105). Biochem Biophys Res Commun 1999;265:134–139.
35. van Luyn MJ, van Wachem PB, Damink LO, Dijkstra PJ, Feijen J, Nieuwenhuis P. Relations between *in vitro* cytotoxicity and crosslinked dermal sheep collagens. J Biomed Mater Res 1992; 26:1091–1110.
36. Ishaug SL, Crane GM, Miller MJ, Yasko AW, Yaszemski MJ, Mikos AG. Bone formation by three-dimensional stromal osteoblast culture in biodegradable polymer scaffolds. J Biomed Mater Res 1997;36:17–28.
37. Martin I, Shastri VP, Padera RF, Yang J, Mackay AJ, Langer R, Vunjak-Novakovic G, Freed LE. Selective differentiation of mammalian bone marrow stromal cells cultured on three-dimensional polymer foams. J Biomed Mater Res 2001;55:229–235.
38. Freed LE, Vunjak-Novakovic G. Tissue engineering bioreactors. In: Lanza RP, Langer R, Vacanti J, editors. Principles of tissue engineering. San Diego: Academic Press; 2000. pp 143–156.
39. Betts F, Blumenthal NC, Posner AS, Becker GL, Lehninger AL. Atomic structure of intracellular amorphous calcium phosphate deposits. Proc Natl Acad Sci USA 1975;72:2088–2090.
40. Bonar LC, Grynpas MD, Glimcher MJ. Failure to detect crystalline brushite in embryonic chick and bovine bone by X-ray diffraction. J Ultrastruct Res 1984;86:93–99.
41. Grynpas MD, Bonar LC, Glimcher MJ. Failure to detect an amorphous calcium-phosphate solid phase in bone mineral: a radial distribution function study. Calcif Tissue Int 1984;36: 291–301.
42. Fisher LW, Whitson SW, Avioli LV, Termine JD. Matrix sialoprotein of developing bone. J Biol Chem 1983;258:12723–12727.
43. Lecanda F, Avioli LV, Cheng SL. Regulation of bone matrix protein expression and induction of differentiation of human osteoblasts and human bone marrow stromal cells by bone morphogenetic protein-2. J Cell Biochem 1997;67:386–396.
44. Zhao M, Berry JE, Somerman MJ. Bone morphogenetic protein-2 inhibits differentiation and mineralization of cementoblasts in vitro. J Dent Res 2003;82:23–27.
45. Butler WT. The nature and significance of osteopontin. Connect Tissue Res 1989;23:123–136.